

Rigid lid, quasihydrostatic, and hydrostatic numerical methods

O. B. Fringer and R. L. Street

Environmental Fluid Mechanics Laboratory, Stanford University, Stanford, CA
94305

1 Pressure Splitting

The total pressure can be split into its hydrostatic and hydrodynamic parts, as in

$$p = p_h + q, \quad (1)$$

where p_h is the hydrostatic part associated with barotropic and baroclinic forces and q is the hydrodynamic part associated with pressure changes arising from velocity fluctuations. Accordingly, we can write the hydrostatic part of the pressure as that which solves the hydrostatic equation

$$\frac{\partial p_h}{\partial z} = -(\rho_0 + \rho)g, \quad (2)$$

where ρ_0 is some spatially and temporally constant reference density and ρ contains the perturbation and background densities such that $\rho = \bar{\rho}(z) + \rho'(x, y, z, t)$. Vertical integration of (2) from some depth z to the free surface h yields

$$p(z) = p_s + \rho_0 g(h + r - z), \quad (3)$$

where p_s corresponds to the free surface pressure and r is the hydrostatic pressure arising from the varying density ρ such that

$$r = \int_z^h \frac{\rho}{\rho_0} dz. \quad (4)$$

The gradient of the total pressure is then split into its barotropic, baroclinic, and hydrodynamic parts, respectively, as in

$$\nabla p = \rho_0 g \nabla(h + r) + \nabla q, \quad (5)$$

where p_s is assumed constant.

2 Rigid Lid Algorithm

Writing the pressure as in equation (5) sets the stage for a three level modeling heirarchy, beginning with a computation of the full nonhydrostatic pressure, down to a hydrostatic model. Beginning with the full nonhydrostatic model, the discretized Boussinesq equations can be written with a time-centered pressure projection type method [1] where the predictor velocity field is determined with

$$\begin{aligned}\frac{\mathbf{u}^* - \mathbf{u}^n}{\Delta t} &= \mathbf{S}_H^{n+\frac{1}{2}} \\ \frac{w^* - w^n}{\Delta t} &= S_V^{n+\frac{1}{2}} - \frac{\rho^{n+\frac{1}{2}}}{\rho_0} g,\end{aligned}\tag{6}$$

and corrected with the total pressure, which consists of the hydrostatic and hydrodynamic pressures, as in

$$\begin{aligned}\frac{\mathbf{u}^{n+1} - \mathbf{u}^*}{\Delta t} &= -\frac{1}{\rho_0} \nabla \tilde{p}^{n+1} \\ \frac{w^{n+1} - w^*}{\Delta t} &= -\frac{1}{\rho_0} \frac{\partial \tilde{p}^{n+1}}{\partial z}.\end{aligned}\tag{7}$$

All the non-buoyancy and non-pressure terms have been lumped into the right hand side in $\mathbf{S} = (\mathbf{S}_H, S_V)$. Here, the velocity components are split into their horizontal and vertical parts such that the horizontal velocity vector is given by $\mathbf{u} = u\hat{i} + v\hat{j}$, and the gradient operator represents $\nabla = \hat{i}\frac{\partial}{\partial x} + \hat{j}\frac{\partial}{\partial y}$. By enforcing continuity at the $n + 1$ time step such that

$$\nabla \cdot \mathbf{u}^{n+1} + \frac{\partial w^{n+1}}{\partial z} = 0,\tag{8}$$

we can derive a Poisson equation for the total pressure \tilde{p}^{n+1} in terms of the divergent velocity field (\mathbf{u}^*, w^*) by imposing condition (8) on equations (7) to obtain

$$\nabla^2 \tilde{p}^{n+1} + \frac{\partial^2 \tilde{p}^{n+1}}{\partial z^2} = \frac{1}{\Delta t} (\nabla \cdot \mathbf{u}^* + \frac{\partial w^*}{\partial z}).\tag{9}$$

In actuality this pressure \tilde{p}^{n+1} is not the real pressure, but rather is only a first order in time approximation to p^{n+1} [2]. Its sole purpose is to impose continuity at time step $n + 1$. Methods of computing the actual pressure can be found in [1], but in general the real pressure is rarely needed unless

hydrodynamic forces are of interest in the calculation. The evolution of the density field is computed with transport equations for salinity and temperature and a suitable equation of state for density, $\rho = \rho(s, T)$. The free surface dynamics are computed with a kinematic free surface boundary condition of the form

$$\frac{\partial h}{\partial t} + \mathbf{u} \cdot \nabla h = w|_{z=h}, \quad (10)$$

the details of which can be found in [3]. In that work the free surface dynamics are computed explicitly with a higher order time stepping scheme. Equations (6) - (10) constitute a full nonhydrostatic algorithm for geophysical flows. Its main drawback is the Courant condition associated with the explicit calculation of free surface waves, which imposes a severe time step stability restriction.

3 Quasihydrostatic Algorithm

A split nonhydrostatic algorithm, such as that derived by Casulli [4], alleviates the stability limitation associated with fast free surface gravity waves. This is done by using the decomposition (3) in the predictor step (6) so that the predicted horizontal velocity field is forced by the barotropic and baroclinic pressures:

$$\begin{aligned} \frac{\mathbf{u}^* - \mathbf{u}^n}{\Delta t} &= \mathbf{S}_{H'}^{n+\frac{1}{2}} - g\nabla[\theta h^{n+1} + (1 - \theta)h^n] - g\nabla r^{n+\frac{1}{2}} \\ \frac{w^* - w^n}{\Delta t} &= S_V^{n+\frac{1}{2}}, \end{aligned} \quad (11)$$

where we have discretized $h^{n+\frac{1}{2}}$ with a theta method such that $h^{n+\frac{1}{2}} = \theta h^{n+1} + (1 - \theta)h^n$. This velocity field is then corrected with the hydrodynamic pressure, as in

$$\begin{aligned} \frac{\mathbf{u}^{n+1} - \mathbf{u}^*}{\Delta t} &= -\frac{1}{\rho_0} \nabla \tilde{q}^{n+1} \\ \frac{w^{n+1} - w^*}{\Delta t} &= -\frac{1}{\rho_0} \frac{\partial \tilde{q}^{n+1}}{\partial z}, \end{aligned} \quad (12)$$

where again, \tilde{q}^{n+1} is a first order in time approximation to the actual hydrodynamic pressure q^{n+1} . However, $\nabla \tilde{q}^{n+1}$ is approximately an order of magnitude smaller than $\nabla \tilde{p}^{n+1}$ and indeed $\nabla \tilde{q}^{n+1} \approx 0$ over all hydrostatic regions of the

flow. The continuity equation (8) is integrated over the depth to obtain the depth-averaged continuity equation which is exact and, with the use of the kinematic boundary condition (10), becomes

$$\frac{\partial h}{\partial t} + \nabla \cdot \int_{-d}^h \mathbf{u} \, dz = 0. \quad (13)$$

Equation (13) is discretized with a theta-method such that the free surface is computed at the next time step with

$$\frac{h^{n+1} - h^n}{\Delta t} + \theta \nabla \cdot \int_{-d}^{h^n} \mathbf{u}^* \, dz + (1 - \theta) \nabla \cdot \int_{-d}^{h^n} \mathbf{u}^n \, dz = 0. \quad (14)$$

An implicit equation for the free surface at time step $n + 1$ can be obtained through a substitution of \mathbf{u}^* from equations (11) into equation (14). The new free surface can then be found and the predicted velocity fields are obtained through the use of equations (11). Continuity is enforced through a corrector step (12) after solving for the hydrodynamic pressure with

$$\nabla^2 \tilde{q}^{n+1} + \frac{\partial^2 \tilde{q}^{n+1}}{\partial z^2} = \frac{1}{\Delta t} (\nabla \cdot \mathbf{u}^* + \frac{\partial w^*}{\partial z}). \quad (15)$$

The drawbacks to this method are that it requires the solution of two elliptic equations, namely, the 2-D free surface equation for h^{n+1} and the 3-D hydrodynamic pressure equation for \tilde{q}^{n+1} . But since the hydrodynamic pressure gradient $\nabla \tilde{q}$ is smaller by an order of magnitude than the total pressure gradient $\nabla \tilde{p}$, the solution of the 3-D poisson equation for \tilde{q} is much cheaper than it is for \tilde{p} . Moreover, gains associated with eliminating the gravity wave stability condition outweigh the increased computational cost of a second elliptic equation.

4 Hydrostatic Algorithm

A hydrostatic solution is obtained through the use of equation (11) after solving for the free surface implicitly with the use of equation (14). Now, however, the velocities are not corrected with the use of equation (12). Instead, nonhydrostatic pressure effects are neglected and the new velocity field is obtained with the use of the continuity equation, as in

$$\mathbf{u}^{n+1} = \mathbf{u}^*, \quad w^{n+1} = - \int_{-d}^z \nabla \cdot \mathbf{u}^{n+1} \, dz. \quad (16)$$

The hydrostatic algorithm eliminates the need to solve the 3-D elliptic equation for the nonhydrostatic pressure, and hence is very attractive when solving flows under strong hydrostatic balance. It represents an equivalent algorithm to the POM, except that here we solve for the free surface dynamics implicitly and advance the baroclinic and barotropic modes with the same time step.

5 Numerical Comparison

Figure (1) depicts the failure of the hydrostatic model to depict the overturning billows resulting from a Kelvin-Helmholtz instability in a lock exchange flow. These flows were initialized with a hyperbolic tangent horizontal salinity profile with a salinity difference of 4.28 ppt and the heavier fluid to the left of center. While the hydrostatic model correctly depicts the position of the front, it is incapable of capturing the instability that generates the overturning waves. Instead, the hydrostatic model smooths out the front and generates short horizontal waves at the interface. This indicates that a hydrostatic model would not be able to capture overturning mechanisms that lead to a cascade to higher frequencies regardless of how well resolved it was. While not all energy transport to higher modes results from internal wave overturning, this example presents compelling motivation to use a nonhydrostatic model, as it points out a severe limitation that can result from using a hydrostatic code.

References

- [1] Y. Zang, R. L. Street, and J. R. Koseff, A non-staggered grid, fractional step method for the incompressible Navier-Stokes equations in curvilinear coordinates. *J. Comp. Phys.* **114** (1994) 18-33.
- [2] S. W. Armfield and R. L. Street, Time accuracy of fractional-step methods for the Navier-Stokes equations on non-staggered grids. Working Paper (1998).
- [3] B. R. Hodges, *Numerical Simulation of nonlinear free-surface waves on a turbulent open-channel flow*. Ph. D. Diss., Dept. Civil Engineering, Stanford University, 235 pages.
- [4] V. Casulli, Numerical simulation of 3D quasi-hydrostatic free-surface flows. *J. Hyd. Eng.* **124** (1998) 678-686.

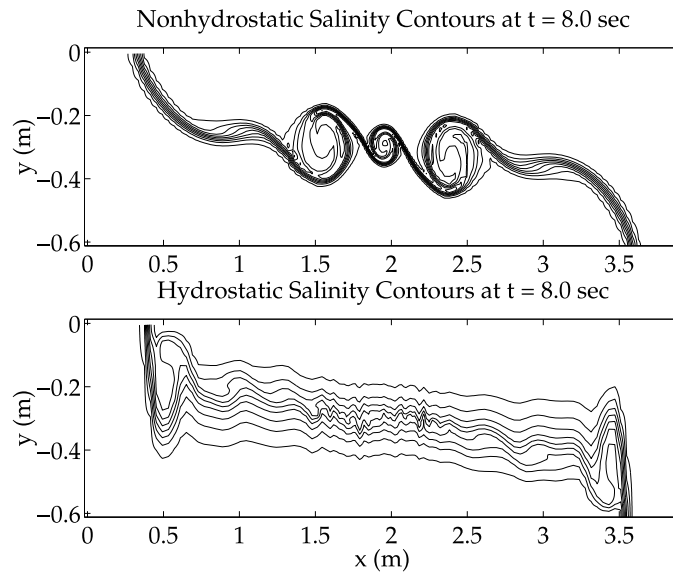


Figure 1: Comparison of the nonhydrostatic and hydrostatic solutions to the lock exchange problem 8 seconds after release of the lock. The shear instability that results in the Kelvin-Helmholtz billows is highly nonhydrostatic, and as a result no waves form for the hydrostatic case.